The photochemical transformation and tautomeric composition of matrix isolated benzotriazole †

Mariusz Kiszka,[a,b] Ian R. Dunkin,*[a] Jerzy Gębicki,[b] Hong Wang[c] and Jakob Wirz[c]

[a] *Department of Pure and Applied Chemistry, University of Strathclyde, Thomas Graham Building, 295 Cathedral Street, Glasgow, UK G1 1XL*
[b] *Institute of Applied Radiation Chemistry, Technical University, Zeromskiego 116, 90-924 Łódź, Poland*
[c] *Institut für Physikalische Chemie, Universität Basel, Klingelbergstrasse 80, CH-4056 Basel, Switzerland*

Received (in Cambridge, UK) 17th August 2000, Accepted 29th September 2000
First published as an Advance Article on the web 6th November 2000

Photolysis of benzotriazole isolated in argon and nitrogen matrices at 12–14 K has been studied by means of UV–visible and IR absorption spectroscopy. Short wavelength irradiation resulted in N–NH bond scission to give diazoimine **3** and minor products: cyanocyclopentadiene **6** and ketenimine **5**. The compound **3** was easily bleachable. With 420 nm light, the major pathway was cycloreversion to benzotriazole, but at shorter wavelengths photolysis of **3** led first to the ketenimine product and ultimately to cyanocyclopentadiene. The photoproducts were identified by means of their characteristic IR absorptions. Identification of **3** was additionally supported by comparison of experimental and computed IR transitions, which also indicated that **3** was generated predominantly as its *E* isomer. Detailed analysis of the benzotriazole IR spectra recorded prior to and after photolysis pointed towards the co-existence of both tautomeric forms, 1*H*-benzotriazole (**1**) and 2*H*-benzotriazole (**2**), frozen from the gas phase during matrix deposition. An estimate of 1.6 : 1 was obtained for the gas-phase [1*H*] : [2*H*] ratio at *ca.* 315 K, in fair agreement with another recent estimate. The benzotriazole tautomers exhibited different photoreactivity, but attempts to utilize this in identifying the IR bands of the individual tautomers were hampered by band overlap, and only a few unequivocal assignments could be made.

Introduction

The tautomerism of benzotriazole

Benzotriazole can exist in two tautomeric forms, 1*H* (**1**) and 2*H* (**2**) (Scheme 1), and the relative stability of these two forms has been extensively studied both experimentally and theoretically.[1–10] Also, the photochemical and thermal transformations of benzotriazole exhibit several interesting reaction patterns yet to be fully understood.[11–16]

Early experimental and computational studies indicated the 1*H* tautomer (**1**) to be the more stable.[1] Crystallographic measurements showed that solid benzotriazole exists almost exclusively as the 1*H* tautomer.[2] Mass spectrometry investigations,[3] spectroscopic studies in various solvents,[4] as well as analysis of microwave[5] and electronic absorption[6] spectra, confirmed the predominance of the 1*H* tautomeric form.

A few of the more recent studies, however, have suggested that the 2*H* tautomer (**2**) may be the more stable.[7–10] Investigations of the temperature effect on the gas-phase electronic absorption spectra of benzotriazole, as well as 1- and 2-methylbenzotriazoles, indicated that the equilibrium favours the 2*H* tautomer.[7] Spectroscopic studies of benzotriazole in jet-cooled molecular beams showed the presence of either only the 2*H* tautomer[8,9] or both tautomeric forms of benzotriazole.[10] Finally, a recent analysis of rotational band contours of the N–H stretching vibration at six different temperatures[17] has led to the conclusion that the 1*H* tautomer is stabilized with respect to the 2*H* tautomer, but only by 5 kJ mol^{-1}.

Failure to detect the 2*H* tautomer of benzotriazole in the microwave spectrum[5] was very probably due to its possessing a much lower dipole moment than the 1*H* tautomer. Dipole moments for 1*H*- and 2*H*-benzotriazole have been estimated theoretically, and are predicted to lie in the ranges 4.09–4.65 and 0.30–0.77 D, respectively.[7] Comparison can also be made with the non-benzannelated analogue, 1,2,3-triazole, for which the experimentally determined dipole moments are 4.38 and 0.218 D for the 1*H* and 2*H* tautomers, respectively.[18]

The photochemistry of benzotriazole

While the 2*H* tautomer of benzotriazole is considered to be relatively stable photochemically, the 1*H* tautomer certainly can undergo light-induced transformations.[11] The potential applications of benzotriazole photoreactivity are well illustrated by the recent development of a new class of light-activatable DNA cleaving agents containing the benzotriazole group.[12] The cleaving action is based on photoinducible nitrogen–nitrogen bond breaking in the triazole ring, followed by nitrogen loss. The resulting carbenes or radicals are then capable of hydrogen abstraction and thereby serve as potential agents for DNA cleavage. It has been pointed out, however, that photolysis of benzotriazole in solution tends to give poor yields of isolable products from nitrogen elimination and that this application is therefore remarkable.[16]

The primary intermediate produced by the N–NH bond scission is expected to be the diazoimine compound **3**, as shown in Scheme 1. This intermediate was first recognized experimentally by an electronic absorption with λ_{max} at 423 nm and a characteristic, broad ν(CNN) absorption in the IR, with a maximum at 2070 cm^{-1}, both of which arose during 254 nm photolysis of benzotriazole in an EPA glass at 77 K (EPA is a mixture of diethyl ether, isopentane and ethanol).[13] The UV

† Details of the B3LYP/6-31G* computations of IR transitions of **1** and **2**, reported in ref. 9, and of **3**, carried out as part of this work, are available as supplementary data. For direct electronic access see http://www.rsc.org/suppdata/p2/b0/b006754g/

 DOI: 10.1039/b006754g

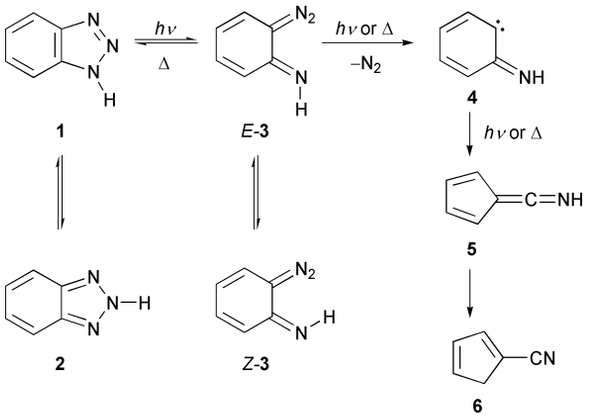

Scheme 1

and IR absorptions were bleached by subsequent irradiation of the glass with 420 nm light, but no other IR bands belonging to **3** were recorded at that time, no doubt because of strong solvent and cell-window absorptions. In contrast, broad band photolysis ($\lambda > 300$ nm) of benzotriazole in an argon matrix at 10 K apparently did not give rise to detectable amounts of **3**,[19] presumably owing to secondary photolysis.

Although the primary intermediate generated in the course of the photodecomposition of benzotriazole has been identified, the final products of the transformations strongly depend on experimental conditions and, in particular, the reaction medium. In the previous study utilizing Ar matrices,[19] the main product was ketenimine **5** (ν(CCN) at 2044 cm^{-1}); while, in the gas phase,[20] the main product was found to be 1-cyanocyclopentadiene (**6**). On the other hand, in reactive condensed media, such as solutions[21] or low temperature glasses (*e.g.* MeOH–EtOH or EPA at 77 K),[13] various products have been observed, arising either *via* insertion reactions (*e.g.* methoxy- or ethoxyaniline) or *via* hydrogen-atom abstraction (aniline).

The various products obtained from photolysis of benzotriazole can all be rationalized on the basis of Scheme 1. The primary intermediate, diazoimine **3**, is not stable and, depending on the conditions in which it is generated, can undergo facile thermal or photochemical decomposition to give the transient carbene **4** and a nitrogen molecule. This loss of N_2 is an example of the general case observed for the decomposition of diazo compounds.[14,15] Triplet **4** has been detected by means of EPR spectroscopy,[22] but has so far eluded detection by other spectroscopic techniques. In the presence of reactive species, such as protic solvents, **4** can be trapped as insertion or H-abstraction products. Alternatively, **4** may undergo a photochemical or thermal rearrangement, analogous to the Wolff rearrangement, to give ketenimine **5** and ultimately its tautomer **6**.

Very recently it has been shown in one of our laboratories that, at ambient temperature in solution, diazoimine **3** can undergo thermal recyclization to benzotriazole, a process which takes place within a few nanoseconds at room temperature in aprotic solvents.[16] Under these conditions, loss of N_2 is a minor side reaction.

Thus, in the previous studies of the photolysis of benzotriazole, all of the intermediates and products shown in Scheme 1 have been detected spectroscopically, but only in separate experiments under widely differing conditions. Moreover, the diazoimine intermediate (**3**) has been identified solely on the basis of an electronic absorption and its ν(CNN) band in an EPA glass, and a fuller characterization would be desirable.

Matrix isolation as a technique for studying benzotriazole and its photolysis

The issue of the equilibrium between the two tautomeric forms of benzotriazole is an interesting problem for investigation by matrix isolation, a technique from which some advantages are expected. Firstly, owing to the lack of solvent absorptions in typical matrices such as Ar and N_2, more complete IR spectra of the various intermediates and products should be obtainable than in, *e.g.*, organic glasses. Secondly, very rapid condensation of benzotriazole vapour with an excess of an inert gas on the low temperature surface may preserve the tautomer ratio of the equilibrium at, or near, room temperature. In addition, because of the narrow bandwidths and lack of rotational fine structure typical in matrix IR spectra, careful analysis of the spectra of benzotriazole prior to and after photolytic treatment may resolve the characteristic absorption bands which belong to particular tautomeric forms of benzotriazole. Finally, the matrix-isolation technique in conjunction with selective photolysis can be used to study the reactions of isolated benzotriazole molecules in a 'step-by-step' fashion, and thus help to establish the reaction pathways and the ultimate products.

In this paper we report the results of matrix-isolation IR and UV–visible studies of the photolysis of benzotriazole, in which some of the expected advantages of the matrix-isolation technique have been realized.

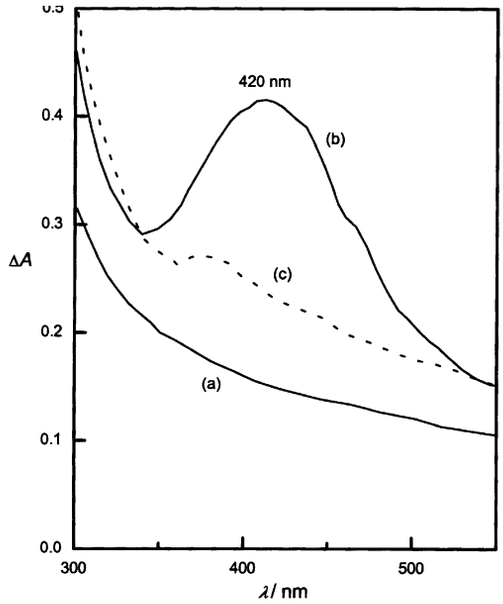

Fig. 1 UV–visible absorption spectra of benzotriazole isolated in an Ar matrix at 12 K: (a) before photolysis; (b) after 4 min photolysis at 254 nm; (c) after subsequent 5 min photolysis at 420 nm.

Results and discussion

Photolyses of benzotriazole in Ar and N_2 matrices have been carried out utilizing low-pressure (254 nm) and unfiltered medium-pressure (wide-band) Hg arcs, and a 248 nm excimer laser. The ensuing processes have been monitored by both UV–visible and IR absorption spectroscopy.

Benzotriazole and its primary photoproduct

UV–visible absorption spectra of benzotriazole isolated in an argon matrix at 12 K, before and after photolysis, are presented in Fig. 1. The most striking spectral feature observed after initial irradiation with 254 nm light was a broad absorption band with a maximum at 420 nm. The species giving rise to this band was very photosensitive and underwent facile bleaching on subsequent illumination at 420 nm. Similar spectra were recorded for nitrogen matrices. These observations are in agreement with results from the photolysis of benzotriazole in an EPA glass,[13] where the observed UV absorption was assigned to diazoimine **3**. No characteristic UV–visible absorption was observed to arise upon bleaching of the 420 nm absorption.

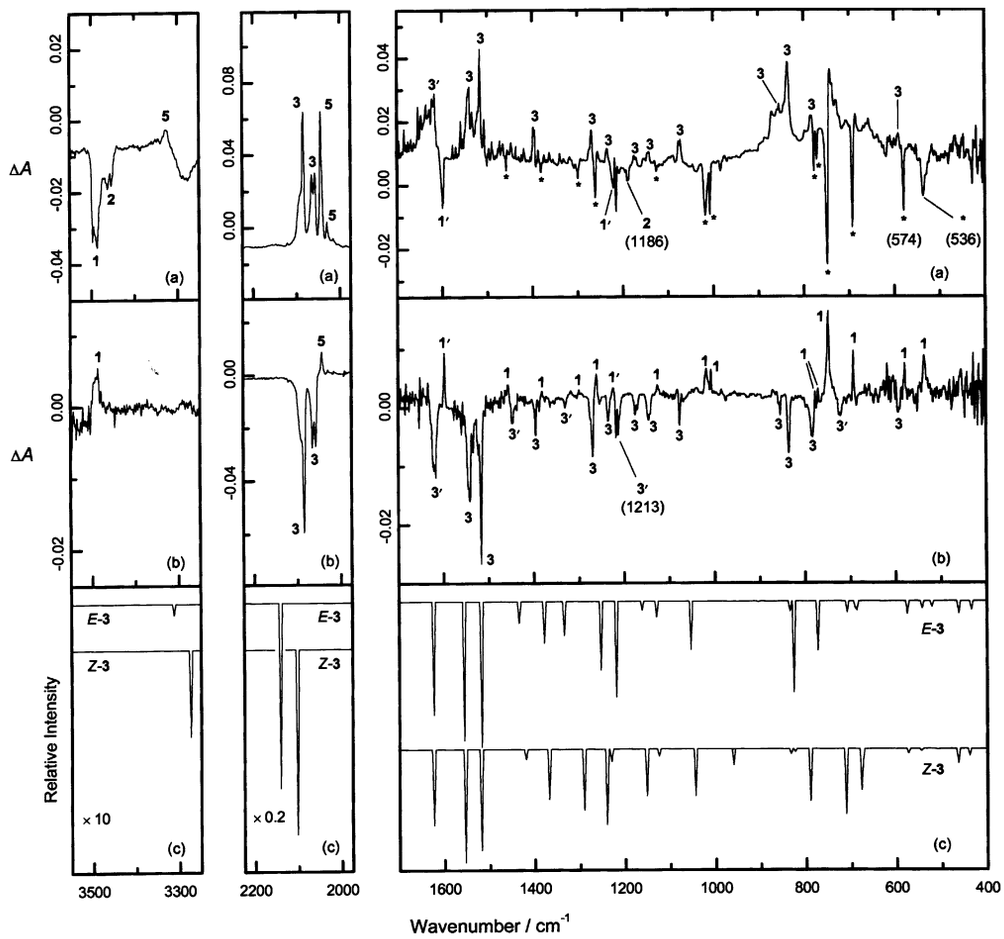

Fig. 2 Selected regions of experimental IR difference spectra and computed IR spectra for *E*- and *Z*-**3**. (a) Difference spectrum showing changes in absorbance after 2 min photolysis of benzotriazole at 254 nm in an argon matrix at 12 K; bands which grew are positive, those which diminished are negative. (b) Difference spectrum obtained following the 254 nm irradiation shown in (a), and after a further 3 min irradiation at 420 nm; bands which grew in the second photolysis are positive, while those which diminished are negative. (c) Simulated IR spectra of *E*- and *Z*-**3** computed using the B3LYP/6-31G* model, and shown with a simulated FWHM of 4 cm^{-1} to aid visual comparison with the experimental spectra. Note that the very strong bands in the region 2200–2000 cm^{-1} are shown at a reduced intensity scale in (a), (b) and (c), and that the computed ν(NH) bands near 3300 cm^{-1} in (c) are shown with 10-fold expansion. Bands assigned to **1**, **2**, **3** and **5** are marked accordingly; those identified with primes are bands with intensities distorted by overlap with others. Bands marked with an asterisk are assigned to either or both of the benzotriazole tautomers (**1** and **2**). See the discussion for an explanation of the band assignments.

In complementary experiments with larger amounts of benzotriazole deposited, the IR bands of benzotriazole were observed in both Ar and N_2 matrices, and these are listed in Table 1. Small differences in band positions and intensities may be attributed to matrix site effects. Assignments of the bands to either **1** or **2** are based mainly on previous DFT calculations (B3LYP/6-31G*),[9] modified in a few cases as a result of our own observations. These are discussed more fully below.

The IR absorptions listed in Table 1 diminished in intensity after the initial photolysis at 254 nm, while a large number of new bands arose, some of which can be seen in Fig. 2(a). Among the new bands were absorptions in the region 2120–2050 cm^{-1}, which could be assigned to a diazo compound,[23] probably diazoimine **3**, and at 2044, 2030 and 2017 (Ar) or 2047, 2022 and 2016 cm^{-1} (N_2), which are equally characteristic for the ketenimine **5**.[19] A very weak single band at 3328 (Ar) or 3329 cm^{-1} (N_2) was also observed, which is assigned as the ν(NH) band of **5**, since it appears not to belong to **3** (see below). In addition, there was a very weak absorption at 2241 cm^{-1} (not shown in Fig. 2(a)), which could be assigned to a cyano group.[23] (The position of this band was found to vary in the range 2241–2234 cm^{-1} in different matrices.) Thus, the matrix photoreaction seems to proceed, at least partially, *via* the pathway leading to cyanocyclopentadiene **6**, *via* **5**, as observed for the gas phase.[20]

Nevertheless, detailed inspection of the matrix IR spectra recorded after partial photolysis of benzotriazole always revealed the presence of very many bands; so numerous product species were probably formed in these conditions. It was possible to identify one sub-set of these product bands, however, because uniquely they diminished in intensity upon subsequent long wavelength irradiation with 420 nm light, and thus followed exactly the behaviour of the broad electronic absorption shown in Fig. 1. The IR bands which arose after 254 nm photolysis and diminished on further 420 nm photolysis were therefore assigned to the species with the 420 nm electronic absorption. They include the strong diazo absorptions near 2100 cm^{-1}, which support the identification of this intermediate as diazoimine **3**. These bands are marked accordingly in the difference spectrum of Fig. 2(b), and all the IR absorptions assigned to **3**, observed in both argon and nitrogen matrices, are listed in Table 2. An excellent agreement between the two matrix hosts was found.

The two sets of bands assigned to **3**—those appearing in Fig. 2(a) and those diminishing in Fig. 2(b)—correspond well with each other in position and relative intensity, except for a few where there was significant overlap with bands of the starting material or other photoproducts; these are marked **3′** in Fig. 2. Most notable of this group is the band at 1213 (Ar) or 1218 cm^{-1} (N_2), which lies very close to a strong absorption of benzotriazole at 1216 or 1215 cm^{-1}. That this band of **3** appears

Table 1 IR absorptions (cm^{-1}) of benzotriazole isolated in argon and nitrogen matrices at 12–14 K

Ar matrices	N_2 matrices	Assignment [a]
3486 vs [b]	3484 s [b]	**1** ν(N–H) [c]
3460 s		**2** ν(N–H) [c]
3452 s	3450 m	**2** ν(N–H) [c]
1625 s	1624 m	**1** matrix splitting ? [c]
1594 m? [d]	1599 m? [d]	**1** ν(N=N) + ν(C=C)
1458 w	1458 w	**1/2** ν(C=C)
	1392 vw	
1381 vw	1381 vw	**1/2**
1299 w	1299 vw	**1/2**
1259 w	1261 w	**1/2**
	1220 w	
1216 s	1215 m	**1**
1186 w	1190 w	**2** [c]
1145 w	1148 vw	**1/2**
1128 w	1133 vw	**1/2** [c]
1122 w	1126 vw	**1/2**
1018 m	1018 w	**1**
1008 m	1007 w	**1**
970 w	970 w	**1/2**
779 w	778 m	**1/2**
769 vw	771 w	**1**
746 vs	748 s	**1/2** δ(C–H)
684 m	692 s	**1/2**
663 vw		
574 m	579 m	**1/2**
536 m	536 m	**1/2**

[a] Except where noted, band assignments are based mainly on the results of the B3LYP/6-31G* calculations reported in ref. 9; bands assigned as **1/2** may belong to either tautomer of benzotriazole or to both. [b] Bands are denoted vs (very strong), s (strong), m (medium), w (weak) or vw (very weak). [c] Band assignment confirmed by results obtained in this work. [d] Relative band intensity uncertain owing to overlap with band of water impurity.

at all in the difference spectrum of Fig. 2(b) shows that it may be even more intense than the band of benzotriazole with almost the same frequency. In any case, its relative intensity in Fig. 2(b) is clearly less than it would be if there were no overlap.

The experimentally observed IR absorptions listed in Table 2 can be attributed to the intermediate diazoimine species **3** for the following reasons. Firstly, the bands at 2120, 2084, 2065 and 2057 (Ar) or 2100, 2090 and 2064 cm^{-1} (N_2) are characteristic of the diazo group.[23] Secondly, the spectra also contain the expected ν(C=N) absorption of the imino group at 1623 (Ar) or 1617 cm^{-1} (N_2).[23] Finally, there is very good agreement between the experimentally observed bands assigned to **3** and those which we have calculated by the B3LYP/6-31G* method,[24,25] and which are presented in Fig. 2(c).

Vibrational frequency and IR intensity calculations were carried out for both the *E* and *Z* isomers of **3**. Although the *E* isomer is the more likely to arise immediately from the ring opening of 1*H*-benzotriazole, either or both geometric isomers could be stabilized in the matrices. As might be expected, the computed frequencies and intensities for the two isomers are similar. Nevertheless, the fit between the observed IR spectrum of **3** and that calculated for *E*-**3** is remarkably good, especially when allowance is made for the reduced intensity of the 1213 cm^{-1} band due to overlap, and is significantly better than the fit between the experimental spectrum and that computed for *Z*-**3** (*cf*. Fig. 2(b) and (c)). We therefore conclude that **3** is probably generated in the matrices predominantly as its *E* isomer. Although the *E* isomer is the expected initial product from photocleavage of **1**, it might also be expected that *E*-**3** would readily revert to benzotriazole, even in a low temperature matrix, and that therefore the *Z* isomer, with its higher energy barrier to recyclization, would be the only geometric isomer likely to survive and be detected. The results, however, indicate that the barrier to recyclization is sufficiently high to allow the *E* isomer to survive.

Table 2 IR bands assigned to diazoimine **3**, arising after 254 nm photolysis of benzotriazole and diminishing after subsequent long wavelength photolysis at 420 nm, recorded in argon and nitrogen matrices at 12 K

Ar matrix $\tilde{\nu}$/cm^{-1}	N_2 matrix $\tilde{\nu}$/cm^{-1}
2120 vw [a,b]	2124 vw [a,b]
	2100 s [b]
2084 vs [b]	2090 vs [b]
2065 s [b]	2064 s [b]
2057 s [b]	
1623 m [c]	1617 m [c]
1541 m	1540 m
1516 m	1516 m
1447 m	1446 w
1395 w	1398 w
1270 m	1270 w
1235 w	1235 w
1213 m	1218 m
1175 w	1174 w
1145 w	1145 w
1076 w	1077 w
855 w	855 w
836 m	836 m
784 w	783 w
722 w	722 w
594 vw	

[a] Qualitative intensities of observed IR bands are denoted as vs (very strong), s (strong), m (medium), w (weak) or vw (very weak). [b] Bands at 2130–2050 cm^{-1} are assigned to ν(CNN) of the diazoimine, and clearly exhibit matrix shifts. [c] ν(C=NH).

With the exception of the bands observed at 1270 (Ar) and 1270 cm^{-1} (N_2), which differ in frequency by about 5% from the most plausible corresponding calculated vibration, all the observed bands agree with the appropriately scaled calculated frequencies to within less than 3%. There is, moreover, a good correlation between observed and calculated IR intensities. In particular, all IR bands of *E*-**3** calculated to have more than 5% of the intensity of the strongest IR band (ν(CNN)) appear in the experimental spectrum. Finally, the ν(NH) band at 3328 cm^{-1} shown arising in Fig. 2(a) does not appear to diminish during subsequent 420 nm photolysis of **3** (*cf*. Fig. 2(b)). Moreover, the calculated intensity of the ν(NH) band of *E*-**3** is extremely small (*cf*. Fig. 2(c)). We thus assign the observed ν(NH) band to **5** rather than to **3**.

Our results represent the fullest characterization of the diazoimine **3** to date. The identification of **3** is now supported by a good agreement between the observed spectra and the calculated IR transitions for its *E* isomer.

Secondary photoproducts

After initial 254 nm photolysis of benzotriazole, illuminating the resulting matrices with 420 nm light led to decay of the diazoimine absorptions accompanied by growth of a number of bands, as seen in Fig. 2(b). The strongest bands growing upon irradiation at 420 nm belonged to the starting material, benzotriazole. So far as we are aware, this photochemical recyclization of diazoimine **3** is reported here for the first time, and seems to be the major photochemical reaction pathway for **3** when irradiated at 420 nm. Nevertheless, some absorptions present in the original benzotriazole spectrum, and which quite clearly diminished on 254 nm irradiation, did not appear to grow again as a result of the irradiation with 420 nm light; while others grew again with different relative intensities. These observations are discussed in the next section.

The bands of ketenimine **5** at 2044 (Ar) or 2047 cm^{-1} (N_2) also grew during 420 nm photolysis of **3**, but only very weakly (*cf*. Fig. 2(a) and (b)). Of the other secondary photoproduct absorptions, some may be due to the expected carbene **4**;

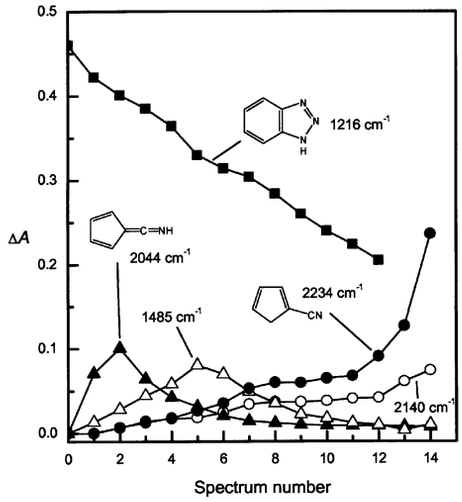

Fig. 3 Evolution of IR band intensities during photolysis of benzotriazole in an Ar matrix with a medium-pressure Hg arc ($\lambda > 200$ nm). Spectra were recorded after photolysis intervals of 1 min initially (Spectrum 1), increasing to 13 min; the total photolysis time was 86 min (Spectrum 14). The species with IR bands at 1485 and 2140 cm^{-1} have not been identified.

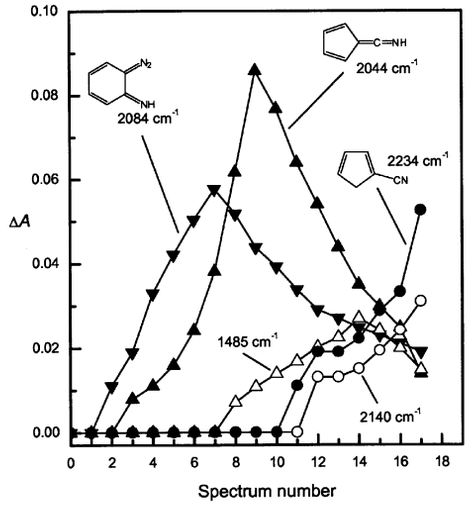

Fig. 4 Evolution of IR band intensities during photolysis of benzotriazole in an Ar matrix with 248 nm laser light. Spectra were recorded after similarly increasing intervals to those used to obtain Fig. 3.

but the IR spectroscopic data do not allow for unequivocal assignments.

In contrast to the IR bands of benzotriazole and **5**, the 2241 cm^{-1} band, which appeared on 254 nm photolysis of benzotriazole and which is assigned to the cyanocyclopentadiene **6**, was not observed to grow further on photolysis of **3** at 420 nm. Therefore, it is reasonable to assume that tautomerization of **5** in low temperature matrices requires the absorption of a further photon with a shorter wavelength than 420 nm. The UV–visible absorption spectrum of **5** is unknown, but the analogous ketene has λ_{max} at *ca.* 260 nm and negligible absorption above 300 nm.[26] It is thus unlikely that ketenimine **5** would be photolysed by 420 nm light.

The experiments involving irradiation of matrices containing **3** with 420 nm light served to distinguish the IR absorptions belonging to **3** from all other photoproduct IR bands and to show that **3** undergoes matrix photolysis at this wavelength to produce mainly recyclized benzotriazole. In turn, these results allow a better understanding of the matrix photolysis of benzotriazole at other wavelengths.

As might be expected, irradiation of benzotriazole in Ar matrices with a 248 nm excimer laser gave results very similar to those described above for 254 nm photolysis using a low-pressure Hg arc. On the other hand, irradiation with the broad band output of an unfiltered medium-pressure Hg arc ($\lambda > 200$ nm) led to a quite distinct evolution of products. In particular, diazoimine **3** was not observed at all from broad band photolysis, in accordance with the previous matrix-isolation study.[19]

Fig. 3 shows the consumption of starting material and the evolution of various products, as monitored by selected IR absorptions, during broad band photolysis of benzotriazole in an Ar matrix. Under these conditions, none of the photolabile diazoimine **3** was detected and the ketenimine **5** was the first intermediate observed. The ketenimine quickly reached a maximum concentration, and underwent secondary photolysis, apparently *via* an intermediate with an IR absorption at 1485 cm^{-1}, to cyanocyclopentadiene (**6**), which appeared stable under the prevailing photolytic conditions.

The intermediate with the 1485 cm^{-1} absorption has not yet been identified. Although cyanocyclopentadiene is simply a tautomer of ketenimine **5**, proton transfer reactions are not favoured in the highly non-polar and extremely low temperature environment of an Ar matrix. Thus the tautomerization requires the absorption of a photon and may proceed *via* an unusual, possibly dissociative, mechanism. On this basis, we considered the cyclopentadienyl radical and the carbene, cyclopentadienylidene, as candidates for the intermediate absorbing at 1485 cm^{-1}; but reported matrix IR spectra of these species do not support either: the radical[27] absorbs at 3079, 1383 and 661 cm^{-1}, while the carbene[26] has its strongest two IR absorptions at 1335 and 703 cm^{-1} and no absorption near 1485 cm^{-1}.

Equally, the photostable product with the IR band at 2140 cm^{-1} has also not been identified. It is possibly an isocyanide isomer of **6**, but it appears to evolve simultaneously with **6**, and not as a result of the photoisomerization of **6**, suggesting that a common intermediate may be involved for both species. This lends further support to the possibility of a dissociative mechanism for the transformation of **5** into **6**. Other obvious possibilities, *e.g.* HCN (ν(CN) 2093 cm^{-1})[28] and HNC (ν(NC) 2029 cm^{-1}),[29,30] do not fit the observed frequency.

Fig. 4 shows similar product evolution profiles for photolysis of benzotriazole in an Ar matrix with 248 nm laser light. The most significant difference from the profiles shown in Fig. 3 is the detection of diazoimine **3** and its secondary photolysis to **5**.

The tautomeric composition of benzotriazole

Among the matrix IR absorptions of benzotriazole, the ν(NH) bands at 3486 cm^{-1} and the pair at 3460 and 3452 cm^{-1} (Ar matrix) were observed to behave in a very interesting way. The relative intensities before photolysis were in the ratio of 1.6:1, but when the sample was irradiated with 254 nm light, the band at 3486 cm^{-1} decreased in intensity more quickly than the pair of bands at 3460 and 3452 cm^{-1}. The relative intensities after 2 minutes photolysis were in the ratio of 1.2:1. Subsequent irradiation at 420 nm, which regenerated the starting material, resulted in re-growth of only the 3486 cm^{-1} absorption (Fig. 2(b)). On the basis of previous frequency calculations at the HF/6-31G* and B3LYP/6-31G* levels of theory[9] and in the light of the more recent band-contour analysis and calculations at the B3LYP/6-311G(d,p) and MP2/6-311G(d,p) levels of theory,[17] the higher frequency band (3486 cm^{-1}) can be assigned to 1*H*-benzotriazole and the lower frequency pair to the 2*H* tautomer.

We have thus shown that both tautomers of benzotriazole are present in the matrices and that the 2*H* form is significantly less photolabile than the 1*H* form. The 2*H* form may simply tautomerize to the 1*H* form on irradiation at 254 nm, but, if so, the 1*H* form is photolysed more quickly than it is generated. We have been unable to observe any distinct photointerconversion of the two tautomers. The UV absorption spectrum of

1-methylbenzotriazole has λ_{max} at *ca.* 248 and 272 nm, that of 2-methylbenzotriazole has λ_{max} at *ca.* 275 nm; while gas-phase benzotriazole has λ_{max} at about 240 and 272 nm.[7] From comparison with the methylated analogues, it seems likely that there is considerable overlap between the UV absorptions of the two tautomers of benzotriazole, except perhaps at shorter wavelengths around 230–250 nm. In our matrix experiments, 248 or 254 nm irradiation of benzotriazole resulted only in the removal of both tautomers. Thus ring cleavage of **1** to give **3** seems to be a much more efficient photoprocess than conversion of **1** into **2**, or **2** into **1**. Unfortunately, light scattering by the matrices prevented us from reliably identifying changes in the UV absorptions at wavelengths below about 280 nm.

On the assumption of comparable extinction coefficients for the N–H bands of the two tautomers, the absorbance ratio for these bands before matrix photolysis gives a measure of the gas-phase equilibrium mixture of benzotriazole at the temperature from which it was deposited (*ca*. 315 K), assuming further that this was frozen during matrix deposition. This absorbance ratio gives an estimate of [1*H*]/[2*H*] = 1.6 at 315 K, which is in satisfactory agreement with the results from the previous band-contour analysis at various temperatures.[17] The tautomer ratio at 315 K derived from that study is 1.4.

In principle, the difference in rates of photolysis of the tautomers **1** and **2** should allow the IR absorptions of each to be distinguished. Therefore, having observed the differences in behaviour of the ν(NH) bands, we looked for similar differences in all the other IR bands of benzotriazole. This search was less fruitful than we had hoped, however, mainly owing to band overlap and the relative weakness of the absorptions of the minor tautomer (**2**).

Results from previous computations suggest that a large proportion of the IR bands of each tautomer of benzotriazole should have counterparts with similar frequencies (within about 10–15 cm^{-1}) and intensities in the spectrum of the other.[9] This seems to be borne out by experiment. Note, for example, the pronounced variation in the bandwidths of the IR absorptions of benzotriazole in Fig. 2, which may be due in part to overlap of the bands of the two tautomers. In Table 1, we have made assignments of the observed bands in the matrix IR spectra of benzotriazole to the individual tautomers **1** and **2**, based on the published computations, and modified in a few cases by our own observations. The majority of the IR bands of matrix isolated benzotriazole cannot be reliably attributed to a single tautomer.

The differential rates of photolysis of **1** and **2** can be seen quite clearly in the case of the strong ν(NH) bands, but much less clearly in the weaker bands elsewhere in the spectrum. Taking into account the many instances of partial overlapping of product and starting material bands and also the possibility of changes in band shape, which often occur in matrix photolyses, we concluded that differences in the rates of diminution of the IR bands of benzotriazole did not provide a reliable guide for the assignment of bands to **1** and **2**. The regeneration of benzotriazole by photolysis of **3**, seemed more promising, however.

As noted above, when **3** was photolysed at 420 nm, the ν(NH) band of **1** appeared to grow, but the corresponding bands of **2** did not. Thus photoregeneration of benzotriazole from **3** appeared to give only the 1*H* tautomer. On this basis, all of the bands of benzotriazole which grew again on 420 nm photolysis of **3** can be assigned to the 1*H* tautomer (Fig. 2(b)). Nevertheless, as indicated in Table 1, in the original IR spectrum of benzotriazole, many of these bands would also have had some contribution from the 2*H* tautomer as well. We therefore looked for bands of benzotriazole that could be attributed only to **2**, and which should not have grown again after photolysis of **3**. From the computations, there appeared to be only two clear candidates: weak bands at 1186 (Ar) or 1190 cm^{-1} (N_2) and at 1128 (Ar) or 1133 cm^{-1} (N_2). As can be seen in Fig. 2(b) (Ar matrix), the 1186 cm^{-1} band did not grow detectably during photolysis of **3**; and since there appears to be no problem with overlap, it can be safely assigned to **2**. The band at 1128 cm^{-1}, however, clearly did grow on photolysis of **3** and must therefore be assigned to **1** or to both benzotriazole tautomers.

Amongst the other bands of benzotriazole, it is possible to see changes in relative intensities between the bands diminishing on photolysis (Fig. 2(a)) and those growing on regeneration (Fig. 2(b)). For example, in Fig. 2(b), the band at 574 cm^{-1} reappears with weaker maximum extinction than the broader band at 536 cm^{-1}, but in Fig. 2(a) these relative intensities are reversed. This probably indicates a higher contribution by **2** to the band at 574 cm^{-1} than to the band at 536 cm^{-1}, and illustrates the difficulties encountered in trying to make firm assignments.

Overall, the attempt to identify the IR bands of the individual tautomers of benzotriazole has resulted in only a few unequivocal assignments. Perhaps a further study with a higher resolution spectrometer, preferably using neon matrices, where interactions between guest and matrix host species are at a minimum, would provide a clearer picture.

Conclusions

Matrix isolated benzotriazole undergoes facile photolysis with 254 or 248 nm light, initiated by N–NH bond cleavage, and yielding the diazoimine **3** (possessing an electronic absorption with λ_{max} = 420 nm) as the primary photoproduct. Other products observed on prolonged irradiation are ketenimine **5** and cyanocyclopentadiene **6**. These three species have been identified by means of IR spectroscopy, but at least one other intermediate, with an IR absorption at 1485 cm^{-1}, is involved in the matrix photoprocesses, and a further photostable product, possibly an isocyanide isomer of **6**, has also been detected. Photolysis of benzotriazole with broad band light (λ > 200 nm) induces complete secondary photolysis of the primary photoproduct (**3**), which is not detected under these conditions.

Diazoimine **3** also undergoes phototransformation when irradiated at the longer wavelength of 420 nm, and the major pathway under these conditions appears to be recyclization to 1*H*-benzotriazole, with formation of ketenimine **5** as a minor pathway. At this wavelength no cyanocyclopentadiene is formed. This phototransformation of **3** into benzotriazole is reported for the first time in this paper, and has allowed the IR bands of **3** to be distinguished from those of the other photoproducts, resulting in a reasonably confident assignment of about 16 or 17 of its vibrational modes. These assignments are well supported by frequency and intensity calculations at the B3LYP/6-31G* level of theory. Moreover, comparison of the experimental IR spectrum with computed spectra for the two geometric isomers of **3** suggests that the matrix isolated species has the *E* configuration. We have thus achieved the fullest characterization of the diazoimine **3** that has been reported so far.

Analysis of the behaviour of the IR bands on initial photolysis and during recyclization of **3** has allowed the 1*H* and 2*H* tautomers of benzotriazole to be distinguished. The 2*H* form is appreciably less photolabile than the 1*H* form, and is not regenerated from **3** on 420 nm irradiation. The absorbance ratio of the N–H stretching bands of the two tautomers, measured after initial matrix deposition, gives an estimate of the gas-phase tautomer ratio at *ca.* 315 K of [1*H*]/[2*H*] = 1.6. This value is in satisfactory agreement with the ratio of 1.4 derived previously from analysis of ν(NH) band contours in the gas-phase spectrum of benzotriazole. Attempts to assign IR absorptions to the individual benzotriazole tautomers were hindered by extensive overlapping of bands, but a few assignments were possible. A further study of the selective regeneration of 1*H*-benzotriazole from **3**, utilizing a spectrometer with higher resolution, could improve this situation.

Experimental

Equipment

The matrix isolation equipment at Strathclyde and at Basel has been described in detail previously.[31–33] For the IR experiments the deposition window was CsBr while the external windows were KBr. In UV–visible measurements the windows employed were CaF_2 and quartz, respectively. The base temperatures of the systems were 12–14 K.

UV–visible spectra were recorded on a Shimadzu UV-250 spectrophotometer, with double monochromator. IR spectra in the range 4000–400 cm^{-1} were recorded on Bomem MB-100 or Perkin-Elmer 1800 FTIR spectrometers at maximum resolutions of 1 and 0.2 cm^{-1}, respectively.

The following short-wavelength photolysis sources were employed. 1. A pair of Vilber Lourmat low-pressure Hg arc lamps (254 nm, 2×4 W); 2. a Gräntzel low-pressure Hg arc (254 nm); 3. a Lambda Physik excimer laser EMG 101 MSC, operated on KrF (248 nm). Photolyses at longer wavelengths were performed with an Oriel 200 W high-pressure Hg arc, fitted with a quartz lens to effect rough collimation, or a Hanau St. 31 medium pressure Hg arc. When narrow band irradiation was required, an Applied Photophysics f/3.4 high-radiance monochromator or appropriate Schott band-pass glass filters were employed.

Materials

Research grade argon was obtained from BOC Ltd. (≥99.9997%) or from Carba AG (≥99.999%) and nitrogen (≥99.994%) from BOC Ltd.; these were used without further purification. Benzotriazole was purchased from Aldrich (≥99%) or Fluka AG (puriss. p.a.) and used without further purification.

Matrix deposition

Matrices containing benzotriazole were prepared by subliming the compound from a glass side-arm warmed to *ca.* 45 °C, while a large excess of the host gas was allowed through a fine needle valve. The matrix host : guest ratio could not be determined using this method. Pronounced variations in the bandwidths of the IR absorptions of matrix isolated benzotriazole were noted, which could have been due in part to molecular aggregation or may simply have reflected the presence of both tautomers. In any case, the degree of molecular isolation achieved was sufficient to allow observation of the reactive intermediates of interest.

Computations

DFT calculations using the B3LYP hybrid functional and the 6-31G* basis set were carried out for *E*- and *Z*-**3** by means of Gaussian 98W (Revision A.7)[24,25] on a 333 MHz Pentium II PC with 256 Mb of RAM. Computed frequencies have been scaled by the standard factor of 0.9614.[25] Spartan Pro v1.0.3 (Wavefunction, Inc.) was used as a graphic interface for the Gaussian program; structures were initially built in Spartan Pro and were transferred between the two programs in Brookhaven data format (.pdb).

Acknowledgements

We thank the University of Strathclyde and the Technical University of Łódź for an exchange scholarship for M. K., the Swiss National Science Foundation for support, and the EPSRC for equipment grants (GR/H29018 and GR/L61972). We also thank Professor Claus Nielsen for helpful discussions and a referee for suggesting several worthwhile improvements to the paper, including the format for Fig. 2.

References

1 F. Tomás, J.-L. M. Abboud, J. Laynez, R. Notario, L. Santos, S. O. Nilsson, J. Catalán, R. M. Claramout and J. Elguero, *J. Am. Chem. Soc.*, 1989, **111**, 7348.
2 P. A. Escande, J. L. Galigne and J. Lapasset, *Acta Crystallogr., Sect. B*, 1974, **30**, 1490.
3 A. Maquestiau, Y. van Haverbencke, R. Flammang, M. C. Pardo and J. Elguero, *Org. Mass Spectrom.*, 1973, **7**, 1267.
4 H.-U. Schütt and H. Zimmermann, *Ber. Bunsenges. Phys. Chem.*, 1963, **67**, 54.
5 B. Velino, E. Cane, L. Gagliardi, A. Trombetti and W. Caminati, *J. Mol. Spectrosc.*, 1993, **161**, 136.
6 E. Cane, A. Trombetti and B. Velino, *J. Mol. Spectrosc.*, 1993, **158**, 399.
7 F. Tomás, J. Catalán, P. Peréz and J. Elguero, *J. Org. Chem.*, 1994, **59**, 2799.
8 G. Berden, E. Jalviste and W. L. Meerts, *Chem. Phys. Lett.*, 1994, **226**, 305.
9 G. Fischer, X. Cao and R. L. Purchase, *Chem. Phys. Lett.*, 1996, **262**, 689.
10 F. Negri and W. Caminati, *Chem. Phys. Lett.*, 1996, **260**, 119.
11 P. Claus, T. Doppler, N. Galkis, M. Gregoriakis, H. Giezedanner, P. Gilgen, H. Heimgartner, B. Jackson, M. Märky, N. S. Narasimhan, H. J. Rosenkranz, A. Wunderli, H.-J. Hansen and H. Schmid, *Pure Appl. Chem.*, 1973, **33**, 339.
12 P. A. Wender, S. M. Touami, C. Alayrac and U. C. Philipp, *J. Am. Chem. Soc.*, 1996, **118**, 6522.
13 H. Shizuka, H. Hiratsuka, M. Jinguji and H. Hiraoka, *J. Phys. Chem.*, 1987, **91**, 1793.
14 N. J. Turro, *Modern Molecular Photochemistry*, Benjamin–Cummings, Menlo Park, California, 1978.
15 W. Kirmse, *Carbene Chemistry*, 2nd edn., Academic Press, New York, 1971.
16 H. Wang, C. Burda, G. Persy and J. Wirz, *J. Am. Chem. Soc.*, 2000, **122**, 5849.
17 W. Roth, D. Spangenberg, C. Janzen, A. Westphal and M. Schmitt, *Chem. Phys.*, 1999, **248**, 17.
18 M. Begtrup, C. J. Nielsen, L. Nygaard, S. Samdal, C. E. Sjøgren and G. O. Sørensen, *Acta Chem. Scand., Ser. A*, 1988, **42**, 500.
19 H. Tomioka, N. Ichikawa and K. Komatsu, *J. Am. Chem. Soc.*, 1992, **114**, 8045.
20 C. Wentrup and W. D. Crow, *Tetrahedron*, 1970, **26**, 3965.
21 J. H. Boyer and R. Selvarajan, *J. Heterocycl. Chem.*, 1969, **6**, 503.
22 H. Murai, M. Torres and O. P. Strausz, *J. Am. Chem. Soc.*, 1980, **102**, 1421.
23 D. Lin-Vien, N. B. Colthup, W. G. Fateley and J. G. Grasselli, *The Handbook of Infrared and Raman Characteristic Frequencies of Organic Molecules*, Academic Press, Boston, 1991.
24 M. J. Frisch, G. W. Trucks, H. B. Schlegel, G. E. Scuseria, M. A. Robb, J. R. Cheeseman, V. G. Zakrzewski, J. A. Montgomery, Jr., R. E. Stratmann, J. C. Burant, S. Dapprich, J. M. Millam, A. D. Daniels, K. N. Kudin, M. C. Strain, O. Farkas, J. Tomasi, V. Barone, M. Cossi, R. Cammi, B. Mennucci, C. Pomelli, C. Adamo, S. Clifford, J. Ochterski, G. A. Petersson, P. Y. Ayala, Q. Cui, K. Morokuma, D. K. Malick, A. D. Rabuck, K. Raghavachari, J. B. Foresman, J. Cioslowski, J. V. Ortiz, A. G. Baboul, B. B. Stefanov, G. Liu, A. Liashenko, P. Piskorz, I. Komaromi, R. Gomperts, R. L. Martin, D. J. Fox, T. Keith, M. A. Al-Laham, C. Y. Peng, A. Nanayakkara, C. Gonzalez, M. Challacombe, P. M. W. Gill, B. Johnson, W. Chen, M. W. Wong, J. L. Andres, M. Head-Gordon, E. S. Replogle and J. A. Pople, *Gaussian 98W* (Revision A.7), Gaussian, Inc., Pittsburgh, 1998.
25 For a discussion of the B3LYP method applied to the calculation of vibrational frequencies, see W. Koch and M. C. Holthausen, *A Chemist's Guide to Density Functional Theory*, Wiley-VCH, Weinheim, 2000, pp. 130–135.
26 M. S. Baird, I. R. Dunkin, N. Hacker, M. Poliakoff and J. J. Turner, *J. Am. Chem. Soc.*, 1981, **103**, 5190.
27 V. A. Korolev and O. M. Nefedov, *Russ. Chem. Bull.*, 1993, **42**, 1436.
28 C. M. King and E. R. Nixon, *J. Chem. Phys.*, 1968, **48**, 1685.
29 D. E. Milligan and M. E. Jacox, *J. Chem. Phys.*, 1963, **39**, 712.
30 D. E. Milligan and M. E. Jacox, *J. Chem. Phys.*, 1967, **47**, 278.
31 I. R. Dunkin and J. G. MacDonald, *J. Chem. Soc., Perkin Trans. 2*, 1984, 2079.
32 R. Withnall, I. R. Dunkin and R. Snaith, *J. Chem. Soc., Perkin Trans. 2*, 1994, 1973.
33 R. Hochstrasser, PhD Dissertation, Institut für Physikalische Chemie, Universität Basel, 1989.